Rosenbrock-based L-stable Real-Time Method and its partitioned form for Structural dynamic problems

C. Jia, Y. Li, L. Liu, P. Yang and Y. Wu
School of Civil Engineering, Chongqing University, Chongqing, China;
Key Laboratory of New Technology for Construction of Cities in Mountain Area (Chongqing University), Ministry of Education, Chongqing, China

SUMMARY:
Systems of ODEs arising from transient structural dynamics frequently exhibit high-/low-frequency, linear/nonlinear behaviours and mixed first-/second-order forms of subsets of state variables. With this in mind, the paper resorts to the first-order L-stable time integration method, i.e. Rosenbrock-based L-Stable Real-Time(LSRT) method. In detail, a two-stage LSRT (LSRT2) method is introduced, as well as its stability and accuracy analyses via numerical simulations and its application to Real Time Substructuring test of a spring pendulum system. To solve the same problem and to improve computational efficiency, the LSRT2 method is also implemented in a partitioned form and incorporated with subcycling, resulting an interfield parallel time integration method(PLSRT2). To study the numerical performance of the PLSRT2 method, simulations of three-DoF system and Real time substructuring test of a Two-DoF system are carried out. The numerical simulations and the experimental results reveal that the method exhibits favourable stability and second order accuracy.

Keywords: Real-Time Substructuring testing, Rosenbrock method, partitioned integration method,

1. INTRODUCTION

Most of research works carried out on numerical simulations in the field of seismic engineering considers structural integrators for equations of motion second order in time. But for some special cases, such as structural control problems and Real-Time Substructuring Testing(RTST) tests, the utilized integrators are required to deal with mixed first-/second-order ODEs. In order to solve this problem, there are mainly three options: i) to use different integrators for structural and control systems, respectively, –see for instance Wu et al. (2007), that utilizes the Newmark-β method for the emulated structure and a proprietary MTS controller with its own built-in time discretization; ii) to reformulate the control equations in a second-order form (Brüls and Golinval, 2006), and employ a structural integrator like the Generalized-α (Chung and Hulbert, 1993) for both systems; iii) to use first-order integrators like the LSRT algorithms, for both structural and control systems. In this paper, we adopt the last option owing to the fact that it is easier to reformulate second-order ODEs to the first-order form. In addition, the LSRT method exhibits user-defined algorithmic damping, which can filter out high-frequency oscillations without sacrificing the accuracy of low-frequency modes.

As far as complex structures under large excitations are concerned, systems of ODEs may contain high nonlinearity which is frequently concentrated in specific regions of the emulated structures. Hence, both linear Multistep and Runge-Kutta algorithms integrating all state variables, the socalled monolithic way, may impose a huge computational disadvantage for the reason that the used time step is required to satisfy the stability and accuracy conditions of all the state variables. In view of those problems, researchers have devoted significant effort to implement partitioned time integration methods to achieve greater computational efficiency, i.e. integrating different subdomains with different integrators and/or different time steps. Those with different time steps are also called subcycling (Daniel1998) or multi-time-step methods (Gravouil and Combescure 2001). In the framework of multibody system dynamics, Arnold et al. (2003) restricted the communication between subsystems to discrete synchronization points and required interpolation/extrapolation owing to the use of different time steps. They stated that subcycling techniques could suffer from numerical instability that might be further exacerbated by discretization errors introduced by interpolation/extrapolation. To improve stability and/or accuracy, many partitioned integration methods were conceived, including stabilization techniques (Baumgarte1972) and extro/interpolation methods (Daniel1998).

In transient structural dynamics, partitioned methods mainly relied on LMS methods that were applied to the Euler-Lagrange form of equations of motion. A distinct feature of these algorithms was the use of dual unknowns, i.e. the Lagrange multipliers, in order to enforce the continuity between subsystems. By means of a general approach, Gravouil and Combescure solved the system of equations with a structural integrator, i.e. the Newmark scheme (Hughes 1998), thus obtaining a multi-time-step explicit-implicit method (Gravouil and Combescure 2001), hereafter referred to as the GC method. In a greater detail, they conceived a method that was endowed with a conservation law and therefore was spectrally stable. However, the accuracy reduced to first order when subcycling was employed. The energy dissipation of the GC method when subcycling was adopted and the computation of interface reactions at the fine time step in the mesh were considered as drawbacks by Prakash and Hjelmstad (2004), who developed a variant of this method, viz. the PH method, that achieved energy preservation and elimination of interface reactions at the fine time step. Nonetheless, the staggered solution procedures of both the GC and the PH method were considered a drawback in either real-time or parallel computations. In order to solve this issue, Pegon and Magonette proposed an interfield parallel solution procedure complementary to the GC method, which led to a new method, the so-called PM method (Pegon and Pinto 2000). The favourable convergence properties of this method were thoroughly analysed in (Bonelli et al. 2008). Along this line, the paper proposes a novel partitioned integration method with subcycling strategy and parallelism.

2. TWO-STAGE REAL TIME ROSENBROCK-BASED ALGORITHM

Rosenbrock formulas have shown promise in research codes for the solution of initial value problems for stiff systems. These methods are derived from implicit Runge-Kutta methods and employ the Jacobian matrix in simplified Newton iteration for the evaluation of their corresponding implicit formulas. For an ordinary differential equation, either first- or second-order in time, we can write in the more abstract form

$$\dot{\mathbf{y}} = f\left(\mathbf{y},t\right) \quad \mathbf{y}\left(t_0\right) = \mathbf{y}_0 \tag{2.1}$$

To advance the approximate solution of the problem from time t_k to t_{k+1}, an s-stage Rosenbrock method have the form

$$\mathbf{y}_{k+1} = \mathbf{y}_k + \sum_{i=1}^{s} b_i \mathbf{k}_i,\ \left[\mathbf{I} - \gamma_{ii}\Delta t\mathbf{J}\right],\ \mathbf{k}_i = \mathbf{f}\left(\mathbf{y}_k + \sum_{j=1}^{i-1}\alpha_{ij}\mathbf{k}_j, t_k + \alpha_i \Delta t\right)\Delta t + \mathbf{J}\sum_{j=1}^{i-1}\gamma_{ij}\mathbf{k}_j \Delta t. \tag{2.2}$$

Here the constants α_i, α_{ij}, γ_{ij} and b_i are the algorithm coefficients which determine the characteristic of the algorithm, for instance accuracy, stability and real-time compatibility, and $\mathbf{J} = \partial \mathbf{f} / \partial \mathbf{y}$ is the Jacobian matrix calculated at the initial step solution y_k. Each stage of the method consists of a system of linear equations with unknowns k_i and with the inversion of the matrix $\left[\mathbf{I} - \gamma_{ii}\Delta t\mathbf{J}\right]$. We assume that $\gamma_{ii} = \gamma$, so that only one LU-decomposition is needed per step. In order to achieve real-time compatibility, it is assumed that $\alpha_i = \sum_{j=1}^{i-1}\alpha_{ij}$ so that the function f and its derivative at beginning of every inner stage only depend on the known solutions and coupling forces solved before.

Based the form (2.2), Bursi et al. (2008) proposed three LSRT methods. On account of accuracy requirement and ease of implementation, the paper adopt the second order LSRT2 method to develop an partitioned integration method. To realize real-time compatibility, second-order accuracy and L-stability, the following parameters are set as follows:

$$\alpha_2 = \alpha_{21} = 1/2,\ b_1 = 0,\ b_2 = 1,\ \gamma_{21} = -\gamma,\ \gamma = 1 \pm \sqrt{2}/2\ . \tag{2.3}$$

With these values, the LSRT2 method reads:

$$\begin{aligned} \mathbf{k}_1 &= \left[\mathbf{I} - \gamma \Delta t \mathbf{J}\right]^{-1} \mathbf{f}_k \Delta t,\ \ \mathbf{y}_{k+\frac{1}{2}} = \mathbf{y}_k + \frac{1}{2}\mathbf{k}_1, \\ \mathbf{k}_2 &= \left[\mathbf{I} - \gamma \Delta t \mathbf{J}\right]^{-1} \left(\mathbf{f}_{k+\frac{1}{2}} - \mathbf{J}\gamma \mathbf{k}_1 \right) \Delta t,\ \ \mathbf{y}_{k+1} = \mathbf{y}_k + \mathbf{k}_2 \end{aligned} \tag{2.4}$$

To illustrate its application on structural problems, the semidiscrete equations of motion for a nonlinear structure can be expressed in a general form:

$$\mathbf{M}\ddot{\mathbf{u}}(t) + \mathbf{R}\left(\mathbf{u}(t), \dot{\mathbf{u}}(t)\right) = \mathbf{P}(t)\ . \tag{2.5}$$

where $\mathbf{M}$ stands for the mass matrix which is assumed to be symmetric positive definite for simplicity $\mathbf{P}(t)$ and $\mathbf{R}(\mathbf{u}(t), \dot{\mathbf{u}}(t))$ for the vectors of applied and internal forces, respectively. In a FE context, the force vector can be split as $\mathbf{R}(\mathbf{u}, \dot{\mathbf{u}}) = \mathbf{C}\dot{\mathbf{u}} + \mathbf{K}\mathbf{u}$ with a stiffness matrix $\mathbf{K}$, a damping matrix $\mathbf{C}$ and a displacement vector $\mathbf{u}$. Differentiation with respect to time is expressed by a dot, and thus we set $\dot{\mathbf{u}}$ and $\ddot{\mathbf{u}}$ to define the corresponding velocity and acceleration vectors.

In order to implement the first-order integrator, the Euler-Lagrange form of equation of motion (2.5) is required to be transformed into the following Hamilton form:

$$\dot{\mathbf{y}} = \mathbf{f}(\mathbf{y}, t) = \begin{Bmatrix} \dot{\mathbf{u}} \\ \mathbf{P} - \mathbf{R}(\mathbf{u}, \dot{\mathbf{u}}) \end{Bmatrix},\ \mathbf{y} = \begin{Bmatrix} \mathbf{u} \\ \dot{\mathbf{u}} \end{Bmatrix}\ . \tag{2.6}$$

where y is the state vector. When applied to structural systems, the favourable performance of the LSRT2 method with respect to low and high-frequency response can be observed from Fig. 1 where a comparison with the Generalized-α method (Chung and Hulbert, 1993) and the Chang's method (Chang, 2002) is illustrated. Moreover, the method was proved to be energy-decaying via the energy method, which entails favourable stability for solving nonlinear problems (Jia et al.2011).

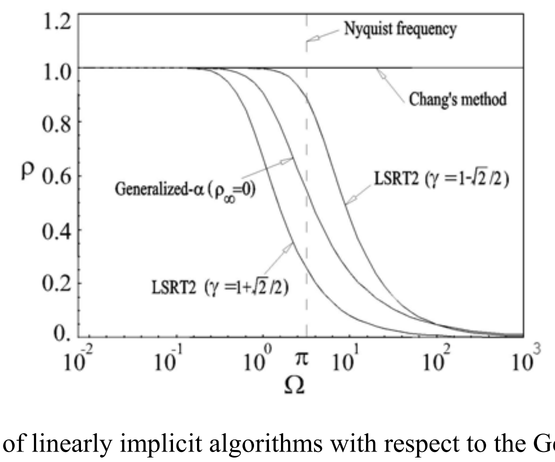

Figure 1. Spectral radii ρ of linearly implicit algorithms with respect to the Generalized-α method and the Chang's method vs. the non-dimensional frequency Ω.

2.1. Numerical simulations of a shear-type structure with a pendulum at the top

To validate the numerical performances of the LSRT2 method, a shear-type structure with a pendulum in Fig. 2 is simulated by means of the LSRT2 method as well as the Constant Average Acceleration method (CAAM). The structural parameters are assumed to be m_1=1.5kg, m_2=10kg, m_3=0.1kg, k_1=k_2=4000N/m, and L=0.2m。 First, we consider free vibration with the initial conditions $\dot{x}_1 = 0.2m/s$, $\dot{x}_2 = 0.1m/s$, $\dot{\theta} = 0.1rad/s$, and the initial displacements are set to be 0. Then, we taken into account forced vibration excited by the N-S component of the Wenchuan earthquake recorded at Shifang whose peak acceleration is scaled to 0.2g. In this case, all the initial values are chosen to be 0. The simulations are realized in Mathematica, the time step is set to be 1ms and $\gamma = 1 - \sqrt{2}/2$ is chosen.

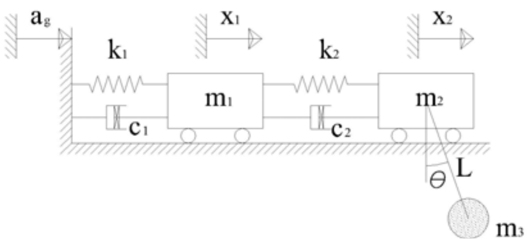

Figure 2. Schematic representation of a shear-type structure with a pendulum at the top

For the sake of brevity, only displacement histories of the first floor and energy histories are presented in Fig. 3 where a reference solution is obtained by means of the LSRT2 method with time step 0.01ms. In the case of free vibration, the displacement solutions of both methods are of great agreement with the reference solution. In the case of excited vibration, the LSRT2 method yields a stable solution while the CAAM method leads to a failure around 7s in the Newton-Raphson iteration of equilibrium as shown in Fig.3(b).

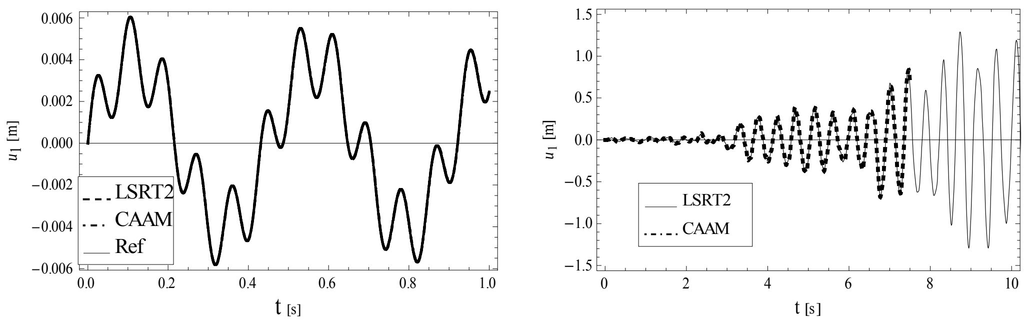

Figure 3. Time history of simulations: (a) displacement under free vibration; (b) displacement under earthquake.

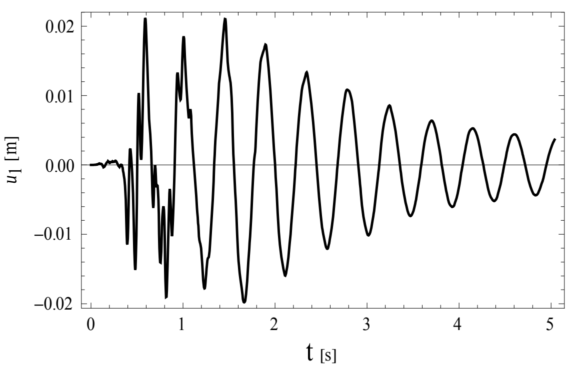

Figure 4. Displacement responses of the first floor of the shear-type structure.

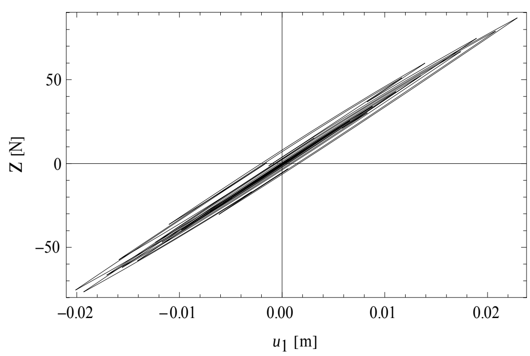

Figure 5. Force-displacement curve for the first storey of the shear-type structure.

In addition, the same structure as shown in Fig. 2 including Bouc-Wen model (Bursi et al. 2011) is also simulated via the LSRT2 method under the E-W component of the Kobe Earthquake. To achieve higher nonlinearity, the peak acceleration is scaled to be 1g. The parameters of the Bouc-Wen model are listed: K_0=4000N/m，$\beta = 5$, $\gamma = 3$ and n=1. The displacement response of the first floor and its hysteretic curve are depicted in Fig. 4 and 5. It is observed that the high-frequency response is dissipated after 1s. This is benefit to the stability of nonlinear simulations including the Bouc-Wen model. Another simulation is done with $\gamma = 1/2$, i.e. without high-frequency dissipation property. The result is unstable which is neglected for sake of simplicity.

2.2. Numerical simulations of a 3-bay 10-storey planer frame structure

To check its applications to finite element models, a 3-bay 10-storey planer frame structure is simulated under the E-W component of the El Centro wave with a peak ground acceleration of 1g. All members are assumed to be constructed from a material with the Young modulus of 30000 MPa and the density of 25kN/m^3. The horizontal displacement of the top story is depicted in Fig. 6 where the reference solution is obtained by the built-in integrator of the Matlab (the lism command). It is observed that the LSRT2 method entails stable result and the result is in high agreement with the reference solution.

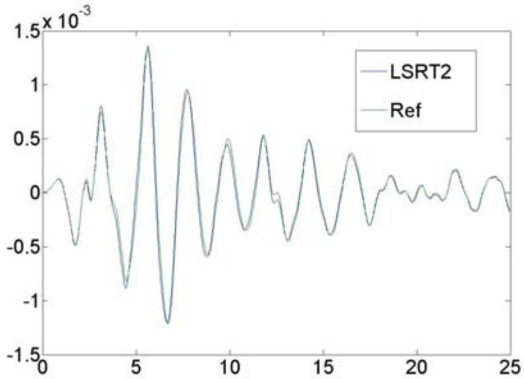

Figure 6. Displacement responses of the top floor of the planer frame structure.

2.3. RTST Test of a spring pendulum structure

In this subsection, the LSRT2 method is applied to a non-linear RTST test. The complete system, the partitioned substructures and the test rig are shown schematically in Fig. 7. It consists of a spring pendulum with its pivot point connected to the mass m_1^p . The pendulum mass, m_2^p , is assumed to act at a single point and is connected to the pivot point by a spring, k_2^p . The parameter values of the system are provided in Table 2.1. In the experiment the Numerical Substructure (NS) is assumed to be nonlinear through a Bouc-Wen model and the behaviour of the 3-DoFs using the LSRT2 method is plotted in Fig. 8. The experimental results show that the capability of the LSRT2 method to deal with nonlinear problems and entails a stable response. Note that the force frequency f=1.2Hz is in resonance with the nonlinear NS.

Table 2.1. Substructure system characteristics.

Numerical model	Phys:cal substructure		External excitation
$M_{1N} = 10$Kg	$M_{1P} = 1$ Kg	$M_{2P} = 0.34$Kg	f = 1.2 Hz, Amp = 20N
$C_{1N} = 40$Kg/s	$C_{1P} = 50$ Kg/s	$C_{2P} = 1.4$Kg/s	Bouc-Wen
$K_{1N} = 1 \times 10^3$N/m	L=0.167m	$K_{2P} = 400$N/m	$\beta - 55$, $\gamma - 45$

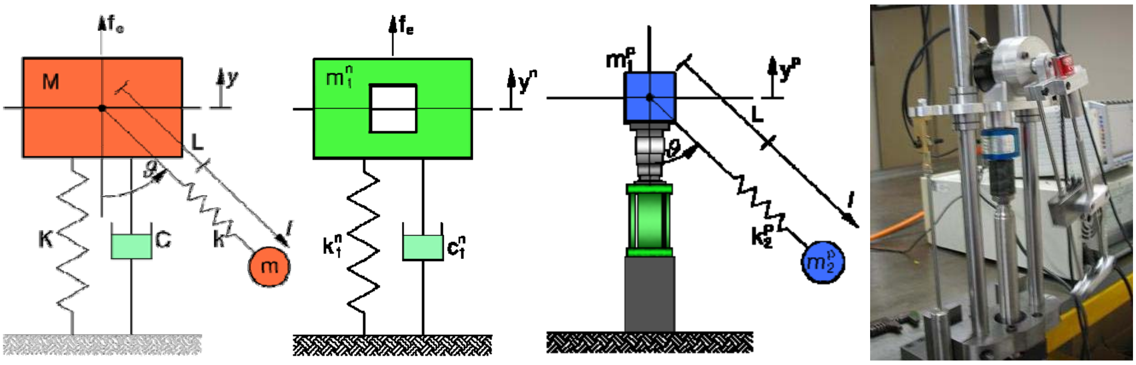

Figure 7. Schematic representation and view of a Three-DoF structure with substructuring.

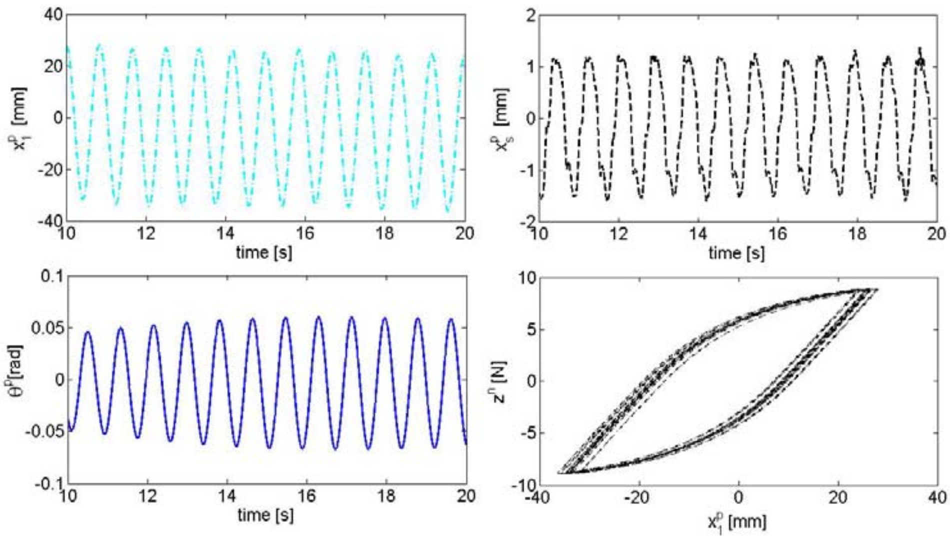

Figure 8. Experimental results of the three-DoF system excited by external force with f=1.2Hz and A=20N using the LSRT2 method.

3. PARTITIONED TIME INTEGRATION METHOD

Systems of ODEs arising from transient structural dynamics, like structure-soil interaction problems or structural control problems, very often exhibit high-frequency/low-frequency and linear/nonlinear behaviours of subsets of state variables, see for instance Fig. 9. In view of those systems, researchers have devoted significant effort to implement partitioned time integration methods to achieve greater computational efficiency. In this section, we present a partitioned time integration method that adopts both the Finite Element Tearing and Interconnection (FETI) method (Farhat et al. 1995) and the LSRT2 method presented in Section 2.

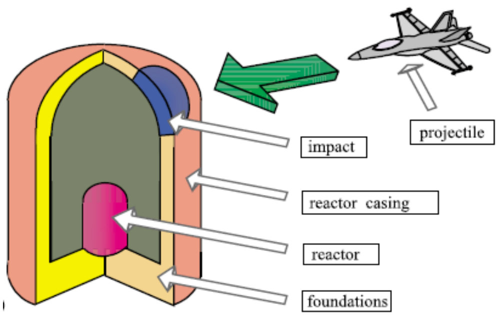

Figure 9. A nuclear reactor vessel under a flight impact.

To ensure real-time compatibility, we consider the acceleration continuity at the interface of subdomains. If the emulated system is divided into two subdomains A and B, the partitioned system can be expressed by a system of Differential Algebraic Equations (DAEs) of index-1

$$\begin{cases} \mathbf{M}_A \ddot{\mathbf{u}}^A + \mathbf{R}^A(\mathbf{u}^A, \dot{\mathbf{u}}^A) = \mathbf{P}^A + \mathbf{G}_A^{\mathrm{T}} \Lambda \\ \mathbf{M}_B \ddot{\mathbf{u}}^B + \mathbf{R}_B(\mathbf{u}^B, \dot{\mathbf{u}}^B) = \mathbf{P}^B + \mathbf{G}_B^{\mathrm{T}} \Lambda \\ \qquad \mathbf{G}_A \ddot{\mathbf{u}}^A + \mathbf{G}_B \ddot{\mathbf{u}}^B = 0 \end{cases} \tag{3.1}$$

To implement the LSRT2 method, the following transformation is required:

$$\begin{cases} \mathbf{A}_A \dot{\mathbf{y}}^A = \mathbf{F}^A + \mathbf{C}_A^{\mathrm{T}} \Lambda \\ \mathbf{A}_B \dot{\mathbf{y}}^B = \mathbf{F}^B + \mathbf{C}_B^{\mathrm{T}} \Lambda \\ \mathbf{C}_A \dot{\mathbf{y}}^A + \mathbf{C}_B \dot{\mathbf{y}}^B = 0 \end{cases} \tag{3.2}$$

where

$$\begin{gathered} \mathbf{A}_A = \begin{bmatrix} \mathbf{I}_A & 0 \\ 0 & \mathbf{M}_A \end{bmatrix}, \mathbf{A}_B = \begin{bmatrix} \mathbf{I}_B & 0 \\ 0 & \mathbf{M}_B \end{bmatrix}, \\ \mathbf{y}^A = \begin{Bmatrix} \mathbf{u}_A \\ \dot{\mathbf{u}}_A \end{Bmatrix}, \mathbf{y}^B = \begin{Bmatrix} \mathbf{u}_B \\ \dot{\mathbf{u}}_B \end{Bmatrix}, \mathbf{C}_A = \begin{bmatrix} 0 \\ \mathbf{G}_A \end{bmatrix}, \mathbf{C}_B = \begin{bmatrix} 0 \\ \mathbf{G}_B \end{bmatrix}, \\ \mathbf{F}^A = \begin{Bmatrix} 0 \\ \mathbf{P}^A - \mathbf{R}^A(\mathbf{u}^A, \dot{\mathbf{u}}^A) \end{Bmatrix}, \mathbf{F}^B = \begin{Bmatrix} 0 \\ \mathbf{P}^B - \mathbf{R}^B(\mathbf{u}^B, \dot{\mathbf{u}}^B) \end{Bmatrix}. \end{gathered} \tag{3.3}$$

Considering Eq. (10), an explicit Lagrange multiplier formulation is obtained

$$\mathbf{\Lambda} = -\mathbf{H}^{-1}\left(\mathbf{C}_A \mathbf{A}_A^{-1} \mathbf{F}^A + \mathbf{C}_B \mathbf{A}_B^{-1} \mathbf{F}^B\right), \quad \text{where } \mathbf{H} = \mathbf{C}_A \mathbf{A}_A^{-1} \mathbf{C}_A^{\mathrm{T}} + \mathbf{C}_B \mathbf{A}_B^{-1} \mathbf{C}_B^{\mathrm{T}}. \tag{3.4}$$

It is just because of the explicit evaluation of $\mathbf{\Lambda}$ that the integration of each subdomain can independently advance as shown in Fig. 10 and the partitioned method can maintain explicit property as the progenitor LSRT2 method.

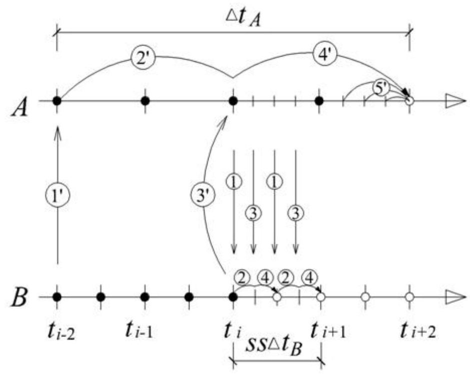

Figure 10. The interfield parallel procedure of the LSRT2-based partitioned method with ss=2.

The solution procedure is highlighted in Fig. 10 and detailed in Table 3.1 with the numbering of the two processes and the subscript i referred to the time step. Subdomain A is integrated with the coarse time step $\Delta t_A = 4 \cdot \Delta t$, while Subdomain B with the fine time step $\Delta t_B = \Delta t / ss$, where $ss = 2$.

The method is not self-starting and to preserve second-order accuracy and parallel characteristics, we choose the LSRT2-based partitioned method (Jia et al. 2011) with no subcycling to initiate the procedure.

Table 3.1. Solution procedure of the PLSRT2 method.

The solution procedure for Subdomain A is as follows:	At the same time, the advancement procedure for substep (j=1⋯ss) in Subdomain B reads:
(1') Evaluate $\mathbf{F}_{i-2}^A$ and $\mathbf{F}_{i-2}^B$ with the solutions $\mathbf{y}_{i-2}^A$ and $\mathbf{y}_{i-2}^B$ and calculate the Lagrange multiplier $\mathbf{\Lambda}_{i-2}$, $\mathbf{\Lambda}_{i-2} = -\mathbf{H}^{-1}\left(\mathbf{C}_A\mathbf{A}_A^{-1}\mathbf{F}_{i-2}^A + \mathbf{C}_B\mathbf{A}_B^{-1}\mathbf{F}_{i-2}^B\right);$ (2') Compute $\mathbf{k}_1^A$ and advance the solution to $\mathbf{y}_i^A$, $\mathbf{k}_1^A = \left[\mathbf{I} - 4\Delta t\gamma\mathbf{J}^A\right]^{-1}\mathbf{A}_A^{-1}\left[\mathbf{F}_{i-2}^A + \mathbf{C}_A^{\mathrm{T}}\mathbf{\Lambda}_{i-2}\right]4\Delta t$ $\mathbf{y}_i^A = \mathbf{y}_{i-2}^A + 1/2\bullet\mathbf{k}_1^A;$ (3') Evaluate $\mathbf{F}_i^A$ and $\mathbf{F}_i^B$ and then calculate $\mathbf{\Lambda}_i$, $\mathbf{\Lambda}_i = -\mathbf{H}^{-1}\left(\mathbf{C}_A\mathbf{A}_A^{-1}\mathbf{F}_i^A + \mathbf{C}_B\mathbf{A}_B^{-1}\mathbf{F}_i^B\right);$ (4') Evaluate $\mathbf{k}_2^A$ and advance the solution to $\mathbf{y}_{i+2}^A$, $\mathbf{k}_2^A = \left[\mathbf{I} - 4\Delta t\gamma\mathbf{J}^A\right]^{-1}\left\{\mathbf{A}_A^{-1}\left[\mathbf{F}_i^A + \mathbf{C}_A^{\mathrm{T}}\mathbf{\Lambda}_i\right] - \gamma\mathbf{J}^A\mathbf{k}_1^A\right\}4\Delta t$ $\mathbf{y}_{i+2}^A = \mathbf{y}_{i-2}^A + \mathbf{k}_2^A;$ (5') Calculate $\mathbf{y}^A_{i+1+\frac{in}{2ss}}$ by means of linear interpolation: $\mathbf{y}^A_{i+1+\frac{in}{2ss}} = \left(1-\frac{in}{2ss}\right)\mathbf{y}_{i+1}^A + \frac{in}{2ss}\mathbf{y}_{i+2}^A$	(1) Evaluate $\mathbf{F}^A_{i+\frac{j-1}{ss}}$ and $\mathbf{F}^B_{i+\frac{j-1}{ss}}$ and calculate $\mathbf{\Lambda}_{i+\frac{j-1}{ss}}$, $\mathbf{\Lambda}_{i+\frac{j-1}{ss}} = -\mathbf{H}^{-1}\left[\mathbf{C}_A\mathbf{A}_A^{-1}\mathbf{F}^A_{i+\frac{j-1}{ss}} + \mathbf{C}_B\mathbf{A}_B^{-1}\mathbf{F}^B_{i+\frac{j-1}{ss}}\right]$ (2) Calculate $\mathbf{k}_1^B$ and advance to $\mathbf{y}^B_{i+\frac{2j-1}{2ss}}$, $\mathbf{k}_1^B = \left[\mathbf{I} - \frac{\Delta t}{ss}\gamma\mathbf{J}^B\right]^{-1}\mathbf{A}_B^{-1}\left[\mathbf{F}^B_{i+\frac{j-1}{ss}} + \mathbf{C}_B^{\mathrm{T}}\mathbf{\Lambda}_{i+\frac{j-1}{ss}}\right]\frac{\Delta t}{ss}$ $\mathbf{y}^B_{i+\frac{2j-1}{ss}} = \mathbf{y}^B_{i+\frac{j-1}{ss}} + \frac{1}{2}\mathbf{k}_1^B$ (3) Evaluate $\mathbf{F}^A_{i+\frac{2j-1}{2ss}}$ and $\mathbf{F}^B_{i+\frac{2j-1}{2ss}}$ and calculate $\mathbf{\Lambda}_{i+\frac{2j-1}{2ss}}$, $\mathbf{\Lambda}_{i+\frac{2j-1}{2ss}} = -\mathbf{H}^{-1}\left[\mathbf{C}_A\mathbf{A}_A^{-1}\mathbf{F}^A_{i+\frac{2j-1}{2ss}} + \mathbf{C}_B\mathbf{A}_B^{-1}\mathbf{F}^B_{i+\frac{2j-1}{2ss}}\right]$ (4) Calculate $\mathbf{k}_2^B$ and advance to $\mathbf{y}^B_{i+\frac{j+1}{ss}}$, $\mathbf{k}_2^B = \left[\mathbf{I} - \frac{\Delta t}{ss}\gamma\mathbf{J}^B\right]^{-1}\left\{\mathbf{A}_B^{-1}\left[\mathbf{F}^B_{i+\frac{2j-1}{2ss}} + \mathbf{C}_B^{\mathrm{T}}\mathbf{\Lambda}_{i+\frac{2j-1}{2ss}}\right] - \gamma\mathbf{J}^B\mathbf{k}_1^B\right\}\frac{\Delta t}{ss}$ $\mathbf{y}^B_{i+\frac{j}{ss}} = \mathbf{y}^B_{i+\frac{j-1}{ss}} + \mathbf{k}_2^B$

3.1. Simulations on a Three-DoF Split Mass system

To investigate the performance of the proposed methods with multiple DoFs at the interface, we consider the Three-DoF system shown in Fig. 11. In the simulations, we consider: E = 2×108kN/m2, I = 2×10-5m4, m_1 =1×104kg, m_2 = 5×103kg, ρ = 2m, r=2, l = 5m. The mass matrices and the stiffness matrices of both subdomains can be defined as:

$$\mathbf{M}_A = \frac{r}{1+r}\begin{bmatrix} m_1 & 0 \\ 0 & \rho^2 m_1 \end{bmatrix},\ \mathbf{M}_B = \frac{1}{1+r}\begin{bmatrix} m_1 & 0 & 0 \\ 0 & \rho^2 m_1 & 0 \\ 0 & 0 & m_2(1+r) \end{bmatrix},\ \mathbf{K}_A = \frac{EI}{l_A^3}\begin{bmatrix} 12 & 6l \\ 6l & 7l^2 \end{bmatrix},\ \mathbf{K}_B = \frac{EI}{l_B^3}\begin{bmatrix} 3 & -3l & -3 \\ -3l & 6l^2 & 3l \\ -3 & 3l & 3 \end{bmatrix} \quad (3.5)$$

The simulations focused on possible drift-off effect at the interface. Time histories of the displacement of the emulated system integrated with Δt=10ms are depicted in Fig.12. One can observe that the partitioned method entail favourable results.

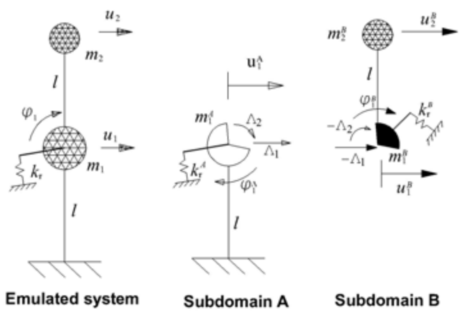

Figure 11. Schematic representation of the Three-DoF split mass structure

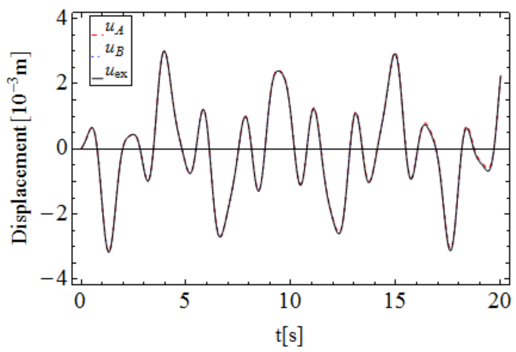

Figure 12. Displacement response of the Three-DoF structure

3.2. RTST Test on Two-Dof split-mass system

In order to validate the effectiveness of the PLSRT2 method in RTST tests, a versatile system was conceived and installed at the University of Trento, Italy. It consists of four actuators, one dSpace DS1103 control board and other high performance devices, shown in Fig.13. This section briefly describes the application of the new parallel method on the 2-Dof split mass system as shown Fig. 14.

Figure 13. Real-Time Substructure testing system and detailed view of a spring.

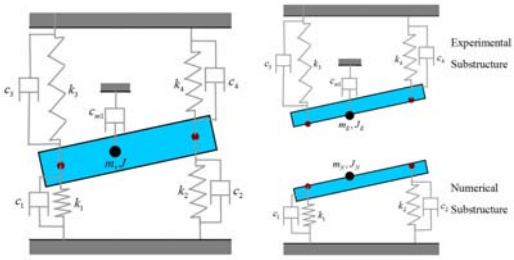

Figure 14. The two-DoF model: (a) emulated system; (b) split system.

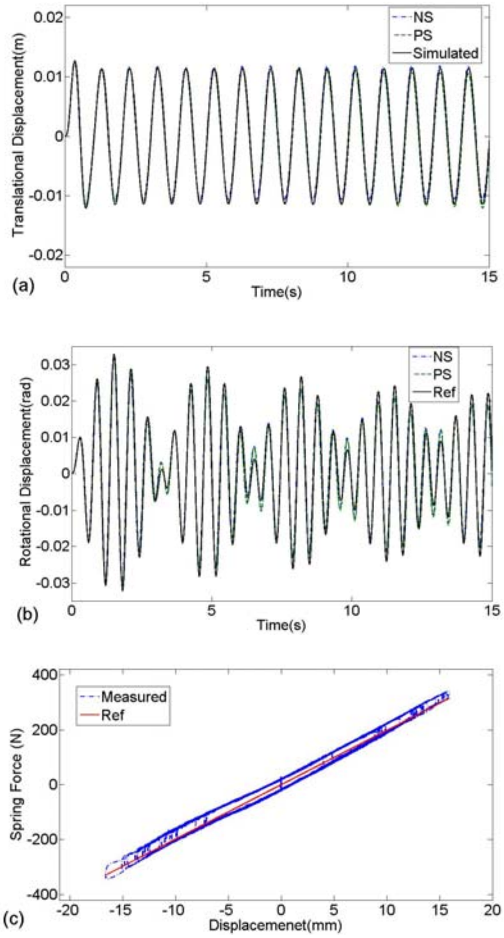

Figure 15. Comparison between experimental and numerical Results.

Table 3.2. Characteristics of both emulated and split subdomains in RTST test

	Emulated system			Numerical substructure			Physical substructure		
Items	M	K	C	M_N	K_N	C_N	M_P	K_P	C_P
Translational	2210.9	346310	555.66	1658.2	306640	555.66	552.7	39670	0
Rotational	157.2	138524	22.226	117.9	12265	22.226	39.3	1711	0

The system characteristics are collected in Table 1. In the test, we selected $\Delta t_A = 4 \cdot \Delta t = 16\text{ms}$ and $\Delta t_B = \Delta t / ss = 2\text{ms}$. Additionally, the system delay of about 20ms was compensated for by means of a polynomial delay compensation scheme (Lamarche et al. 2008). Test results compared with reference numerical simulations are presented in Figure 15. Both displacements fit well to the simulated ones considering the fact that friction forces existing in the system were not modelled. In addition, smaller limited drifts between displacements relevant to both the numerical and the physical substructure were observed.

4. CONCLUSIONS

Initially in this paper, we introduced linearly implicit L-stable Rosenbrock methods with two-stages. And numerical simulations of a planer frame model and RTST test of a spring pendulum system are carried out to validate its numerical performances and applicability to structural dynamic problems. To improve computational efficiency, we developed and illustrated a novel interfield parallel partitioned algorithm. Numerical simulations on a Three-DoF split-mass system are conducted to investigate its stability and accuracy. Moreover a novel test rig conceived to perform both linear and nonlinear substructure tests was introduced, and tests on a two-DoF split-mass system were illustrated. The numerical simulations and the experimental results reveal that the method exhibits favourable stability and second order accuracy. Work in progress is to implement the PLSRT2 method to compensate actuator-induced time delay and to RTST tests of complicated structures.

Acknowledgements:

The paper is supported by Natural Science Foundation Project of Chongqing CSTC (2011BB6077) and the National Key Technology R&D Program (2009BAJ28B01-2). The authors also acknowledge the financial supports from the European Union through the SERIES projects (Grant number: 227887).

REFERENCES

Arnold M., Carrarini A., Heckmann A., and Hippmann, G. (2003). Simulation techniques for multidisciplinary problems in vehicle system dynamics. *Vehicle System Dynamics* **40:1**,17-36.

Baumgarte J. (1972). Stabilization of constraints and integrals of motion in dynamical systems. *Computer Methods in Applied Mechanics and Engineering* **1**,1-16.

Bonelli A., Bursi O. S., He L., Pegon P., and Magonette G. (2008). Convergence analysis of a parallel interfield method for heterogeneous simulations with dynamic substructuring. *International Journal for Numerical Methods in Engineering* **75:7,**800-825.

Brüls, O. and Golinval, J. C. (2006). The generalized-α method in mechatronic applications. *Zeitschrift fur. Angewandte Mathematik und Mechanik* **86:10**,748–758.

Bursi, O. S., Gonzalez-Buelga, A., Vulcan, L. and Wagg, D. J. (2008), Novel coupling Rosenbrock-based algorithms for real-time dynamic substructure testing. *Earthquake Engineering and Structural Dynamics* **37:3**,339-360.

Bursi, O.S., Jia C., Vulcan, L., and Wagg, D. J. (2011). Rosenbrock-based algorithms and subcycling strategies for real-time nonlinear substructure testing. *Earthquake Engineering and Structural Dynamics* **40:1**,1-19.

Chang S. Y. (2002). Explicit pseudodynamic algorithm with unconditional stability. *Journal of Engineering Mechanics* **128:9**,935-947.

Chung, J. and Hulbert, G.M. (1993), A time integration algorithm for structural dynamics with improved numerical dissipation: the generalized-alpha method. *Journal of Applied Mechanics*, **60:2**,371-375.

Daniel W. J. T. (1998). A study of the stability of subcycling algorithms in structural dynamics. *Computer Methods in Applied Mechanics and Engineering* **156:1**, 1-13.

Gravouil A, and Combescure A. (2001). Multi-time-step Explicit-Implicit Method for Non-linear Structural Dynamics. *International Journal for Numerical Methods in Engineering* **50:1**,199-225.

Hughes T.J.R. (1998). The Finite Element Method, Linear Static and Dynamic Finite Element Analysis. Englewood Cliffs, Prentice-Hall, U.K.

Jia C. Bursi, O.S., Bonelli A. and Wang Z. (2011). Novel partitioned integration methods for DAE systems based on L-stable linearly implicit algorithms. *International Journal for Numerical Methods in Engineering* **87:12**,1148-1182.

Lamarche, C. P., Bonelli, A., Bursi, O. S., and Tremblay, R. (2008). A Rosenbrock-W method for real time dynamic substructuring and pseudo-dynamic testing. *Earthquake Engineering and Structural Dynamics* **38:9**,1071-1092.

P. Pegon and A.V. Pinto. (2000). Pseudo-dynamic testing with substructuring applications at the ELSA laboratory. *Earthquake Engineering and Structural Dynamics*, **29:7**,905–925.

Prakash A, Hjelmstad K. D. (2004) A FETI-based multi-time-step coupling method for Newmark schemes in structural dynamics. *International journal for numerical methods in engineering* **61:13**,2183-2204.

Wu, B., Wang, Q., Shing, P.B. and Ou, J. (2007). Equivalent force control method for generalized real-time substructure testing with implicit integration. *Earthquake Engineering and Structural Dynamics* **36:9**,1127–1149.